

## Effect of homogenization time on quench sensitivity of 7085 aluminum alloy

Yu-lin ZHENG<sup>1,2</sup>, Cheng-bo LI<sup>1,3</sup>, Sheng-dan LIU<sup>1,3</sup>, Yun-lai DENG<sup>1,3</sup>, Xin-ming ZHANG<sup>1,3</sup>

1. School of Materials Science and Engineering, Central South University, Changsha 410083, China;

2. Guangxi Alnan Aluminum Inc., Nanning 530000, China;

3. Key Laboratory of Nonferrous Metal Materials Science and Engineering, Ministry of Education, Central South University, Changsha 410083, China

Received 17 October 2013; accepted 23 April 2014

**Abstract:** The effect of homogenization time on quench sensitivity of a cast 7085 aluminum alloy was investigated by means of end-quenching test, optical microscope (OM), scanning electron microscope (SEM) and transmission electron microscope (TEM). The results show that with the increase of homogenization time from 48 h to 384 h, quench sensitivity increased slightly as the largest difference in the hardness was increased from 5.2% to 6.9% in the end-quenched and aged specimens. Prolonging homogenization had little effect on the grain structure, but improved the dissolution of soluble  $T$  phase and resulted in larger  $Al_3Zr$  dispersoids with a low number density. Some small quench-induced  $\eta$  phase particles on  $Al_3Zr$  dispersoids were observed inside grains during slow quenching, which decreased hardness after subsequent aging. The change in the character of  $Al_3Zr$  dispersoids exerted slight influence on quench sensitivity.

**Key words:** 7085 aluminum alloy; homogenization; end quenching; quench sensitivity;  $Al_3Zr$  dispersoids; equilibrium  $\eta$  phase

### 1 Introduction

7000 series aluminum alloys are often called aeronautical materials due to their high specific strength. Recently, it is desirable to fabricate large structural components using thick plates or heavy forgings to meet the rapid development of large aircrafts. 7085 aluminum alloy, which has high strength, high toughness, high corrosion resistance and especially low quench sensitivity [1,2], is a good candidate for these semi-products with large section. For instance, a large 7085 aluminum alloy die forging with a size of 6.4 m×1.9 m has been fabricated successfully and used in Airbus 380 commercial aircraft as inner rear spar.

Generally speaking, 7000 series aluminum alloys are quench sensitive, i.e., slow quenching decreases strength after aging [3,4]. Therefore, thick plates or heavy forgings of these alloys may not be fully hardened due to slow quenching in the middle layer [5]. It is an effective way to solve this problem by decreasing quench sensitivity of these alloys [6]. Quench sensitivity is primarily caused by heterogeneous precipitation of

equilibrium  $\eta$  phase on dispersoids and (sub)grain boundaries during slow quenching, which decreases the supersaturation of both solutes and vacancies, and consequently lower strengthening effect after aging [3–5]. Quench sensitivity receives great effect from microstructure, which is quite complex due to partial recrystallization after solution heat treatment. For instance, in Zr-containing alloy wrought products, there are high angle grain boundaries, subgrain boundaries and  $Al_3Zr$  dispersoids, which are possible heterogeneous nucleation sites of equilibrium  $\eta$  phase during slow quenching [3,7–11]. After recrystallization, some coherent dispersoids may lose coherency with the matrix, and thus become effective heterogeneous nucleation sites; a number of quench-induced  $\eta$  phase particles can often be observed on incoherent  $Al_3Zr$  dispersoids located in recrystallized grains [12]. However, equilibrium  $\eta$  phase was also observed on some dispersoids in subgrains, at subgrain and grain boundaries [3]. All these factors make contribution to high quench sensitivity. But the individual contribution is not clear and difficult to distinguish due to the complex microstructure in the wrought alloys.

Homogenization is an essential step during the production of 7000 series aluminum alloys semi-products. The aim is to dissolve non-equilibrium eutectics, eliminate segregation and precipitate dispersed and small coherent  $\text{Al}_3\text{Zr}$  phase particles in the matrix [13–15]. It was found that homogenization has great effect on the size and distribution of  $\text{Al}_3\text{Zr}$  dispersoids and thus quench sensitivity of a rolled plate of 7050 aluminum alloy [16]. However, it was still difficult to distinguish the effect of dispersoids on the quench sensitivity because of the very different subgrain and grain structure in the plate.

In this work, the effect of homogenization time on the quench sensitivity of a cast 7085 aluminum alloy was investigated. This alloy was homogenized for different time to change the character of  $\text{Al}_3\text{Zr}$  dispersoids without changing grain structure. Therefore, it is likely to find out the effect of  $\text{Al}_3\text{Zr}$  dispersoids alone on quench sensitivity.

## 2 Experimental

The chemical compositions of the studied 7085 aluminum alloy are shown in Table 1. The specimens with dimensions of 125 mm (length)  $\times$  25 mm (width)  $\times$  25 mm (thickness) were cut from an ingot and subjected to homogenization, which included heating slowly to 465 °C, holding for 48 h, 192 h and 384 h, respectively, and then cooling in air. After reheating to 470 °C and holding for 1 h in an air furnace, the specimen was cooled to room temperature by exposing at one end to a vertical stream of cold water [17], then aged at 120 °C in oil bath for 24 h. The aged specimen was evenly cut into two parts, ground and polished, and then the hardness on the center layer was tested along the longitudinal direction. The Vickers hardness testing was performed on a HV-10B hardmeter with a load of 29.4 kN, and five measurements were made at each location to obtain an average value.

**Table 1** Chemical compositions of studied 7085 aluminum alloy (mass fraction, %)

Zn	Mg	Cu	Zr	Fe	Si	Ti	Al
7.52	1.61	1.74	0.11	<0.08	<0.06	<0.05	Bal.

Thin slices at different locations ( $d=3, 78$  mm) from the water-cooled end in the end-quenched specimen were cut for microstructure examination. After grinding and polishing, the slices were etched in the reagent made up of 1 mL HF, 16 mL  $\text{HNO}_3$ , 3 g  $\text{CrO}_3$ , and 83 mL distilled water, and then examined on an XJP-6A optical microscope (OM). The polished samples were also observed on a FEI Quanta-200 scanning electron microscope (SEM) to examine the second phase particles.

Foils of 3 mm in diameter and 0.08 mm in thickness were prepared and electropolished in 20%  $\text{HNO}_3$  + 80%  $\text{CH}_3\text{OH}$  solution below  $-20$  °C, then observed on a FEI Tecnai G<sup>2</sup> 20 transmission electron microscope (TEM) operated at 200 kV to investigate dispersoids and strengthening precipitates.

## 3 Results

### 3.1 Hardness curves

Figure 1(a) shows the influence of homogenization time on the hardness of the end-quenched specimens after aging. Homogenization time had a significant influence on the hardness value. At  $d=3$  mm, the hardness increased obviously with time increasing from 48 h to 192 h, but only slightly from 192 h to 384 h. And over the whole distance, the hardness was higher for the specimens homogenized for 192 h and 384 h than that for 48 h. The shape of the curves was similar, i.e., the hardness decreased with the increase of distance from the water-cooled end. For the specimen homogenized for 48 h, the hardness decreased very rapidly within about 30 mm, but slowly from about 30 mm to about 70 mm, and then tended to be constant with the further increase of distance. For the specimens homogenized for 192 h and 384 h, the hardness decreased rapidly with the distance increasing within about 45 mm and 30 mm, respectively, and then tended to be constant.

Figure 1(b) shows the relationship between the hardness retention value (HRV) and the distance. The hardness retention value was calculated by

$$\text{HRV} = H_x / H_3 \times 100\% \quad (1)$$

where  $H_3$  is the hardness at  $d=3$  mm and  $H_x$  is the hardness at  $d=x$  mm from the water-cooled end. A higher hardness retention value means lower quench sensitivity. The HRV curves exhibit a similar shape to that of the hardness curves, i.e., the value decreased rapidly within a certain distance, which was about 70 mm, 50 mm and 30 mm, respectively, for homogenization time of 48 h, 192 h and 384 h, and then tended to be a constant with the further increase of distance. The highest drop percentage in hardness at  $d=98$  mm was about 5.2%, 6.2% and 6.9%, respectively. This implies that the increase of homogenization time resulted in a slightly higher loss of hardness due to slow quenching, and thus slightly higher quench sensitivity.

### 3.2 Microstructures

Figure 2 shows the optical micrographs of the specimens homogenized for 48 h and 384 h. A number of equiaxed grains could be seen in both specimens, and their size was similar, about 200  $\mu\text{m}$ . Therefore, it is believed that homogenization time had no effect on the amount of grain boundaries in the specimens. Moreover,

some black second phase particles could be identified and most of them were located at grain boundaries.

Figure 3 shows SEM images and typical EDX results of the specimens homogenized for different time. Some bright second phase particles with irregular shape were observed in the specimen homogenized for 48 h, and their size was about 20  $\mu\text{m}$  (see Fig. 3(a)). EDX results show these particles primarily contained Al, Cu and Fe elements with typical content of 73.54%, 8.99% and 17.41% (mole fraction), respectively (particle *A* in Fig. 3(a)). It is likely  $\text{Al}_7\text{Cu}_2\text{Fe}$  phase, which often exists in 7000 series aluminum alloys [18]. It forms during solidification and has high melting temperature, and therefore could not be dissolved by homogenization. Higher magnification image indicated some particles containing Al, Zn, Mg and Cu elements with typical content of 70.09%, 11.05%, 11.22% and 7.04% (mole fraction), respectively (particle *B* in Fig. 3(b)). Therefore, it is likely  $T(\text{AlZnMgCu})$  phase, which often appears in 7000 series Al alloys [19]. In the specimens homogenized for 192 h and 384 h,  $\text{Al}_7\text{Cu}_2\text{Fe}$  phase could still be observed but it is quite difficult to detect *T* phase (Figs. 3(c,d)). Figure 4 shows the area fraction of remnant phase as a function of homogenization time. The results were estimated based on at least five randomly-selected SEM images. With the increase of homogenization time from 48 h to 192 h, a significant

decrease in the area fraction can be seen. This is obviously due to the dissolution of *T* phase. A further increase of time gave rise to almost no change in the area fraction. It is likely because after homogenization of 192 h complete dissolution of *T* phase occurred.

Figure 5 shows typical TEM images of the homogenized specimens. Homogenization time resulted in a large difference in the density, size and distribution of  $\text{Al}_3\text{Zr}$  dispersoids in the matrix.

After homogenization for 48 h and 192 h, there were a number of fine and dispersed  $\text{Al}_3\text{Zr}$  dispersoids (Figs. 5(a) and (b)). According to the non-contrast lines, most dispersoids were coherent with the matrix. After 384 h the density of  $\text{Al}_3\text{Zr}$  dispersoids was lower and their size was larger (Fig. 5(c)). KNIPLING [20] found that in an Al–0.2Zr alloy aged at 425  $^\circ\text{C}$  for 400 h,  $\text{Al}_3\text{Zr}$  dispersoids might lose coherency with the matrix when their radius exceeded about 31 nm. It is believed that many large  $\text{Al}_3\text{Zr}$  dispersoids in Fig. 5(c) were likely incoherent with the matrix according to their morphology and size. Figure 6 shows the size and area fraction of  $\text{Al}_3\text{Zr}$  dispersoids, which were estimated based on at least five TEM images. There was a normal distribution for their radius (Fig. 6(a)); with the increase of homogenization time the mean radius and size difference were increased. The size was quite uniform in the specimens homogenized for 48 h and 192 h, but became

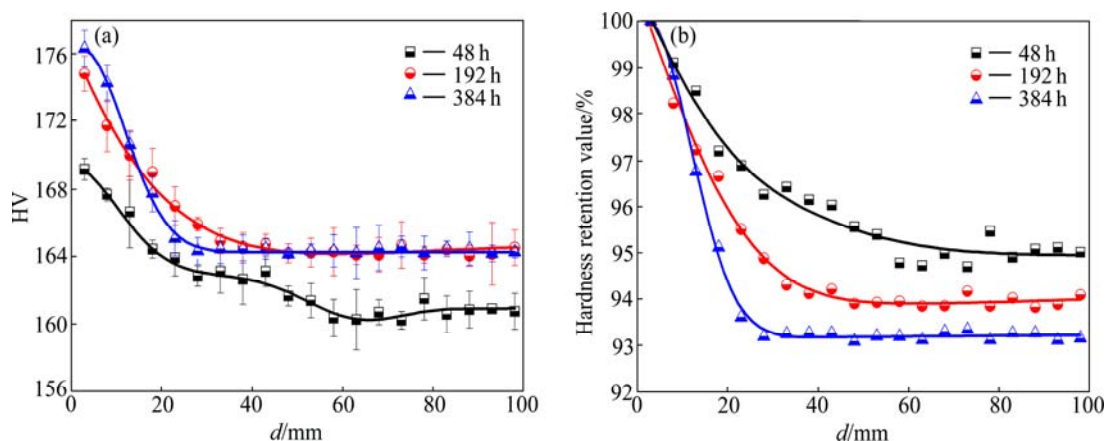


Fig. 1 Influence of homogenization time on hardness (a) and hardness retention value (b) in end-quenched specimen after aging

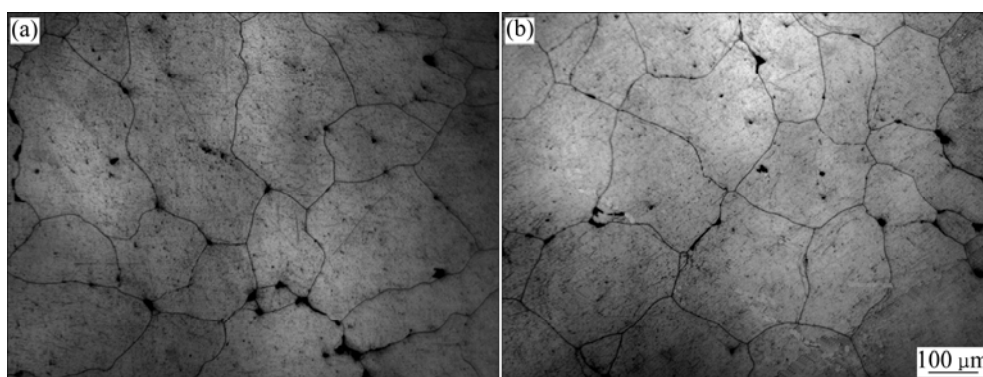
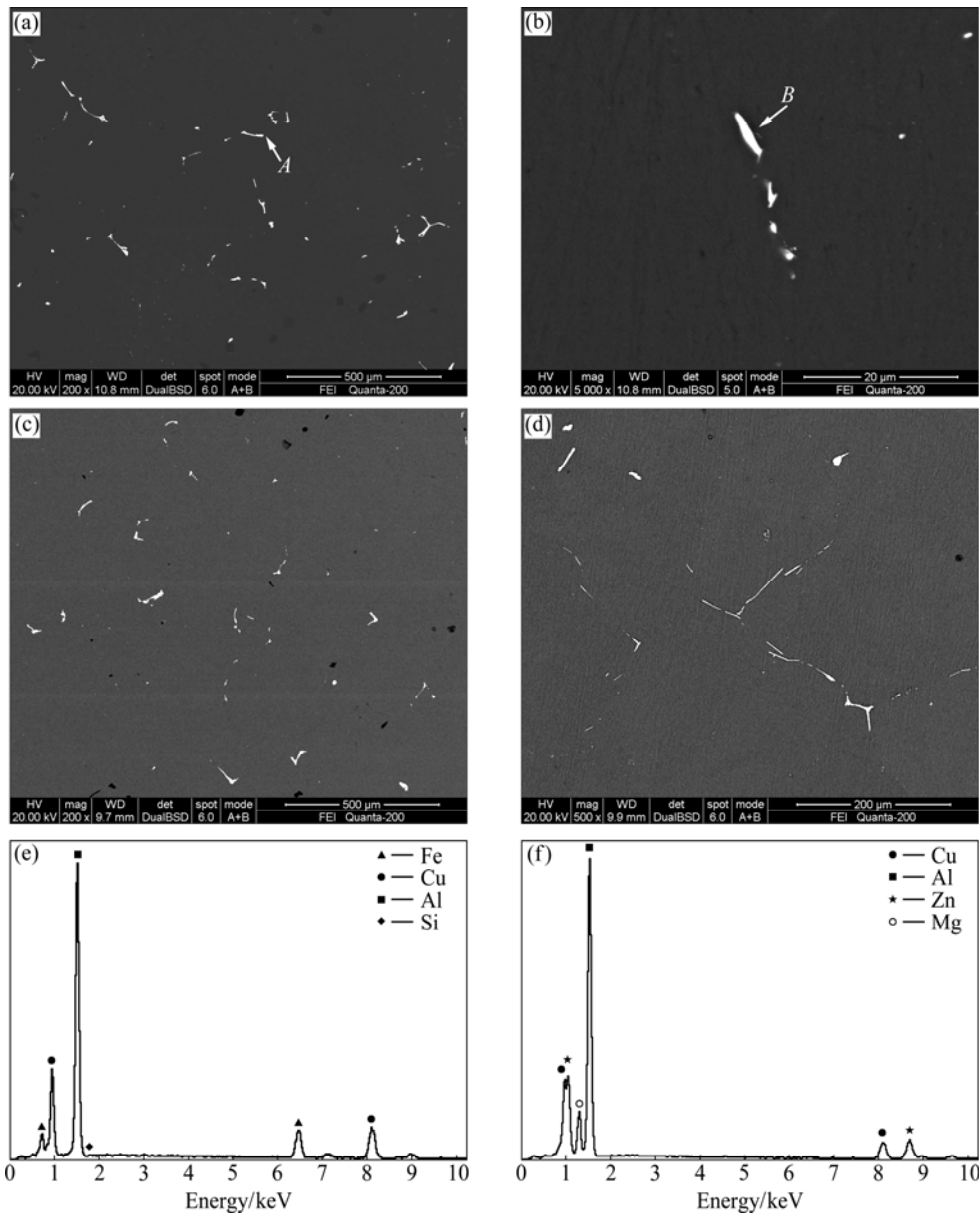
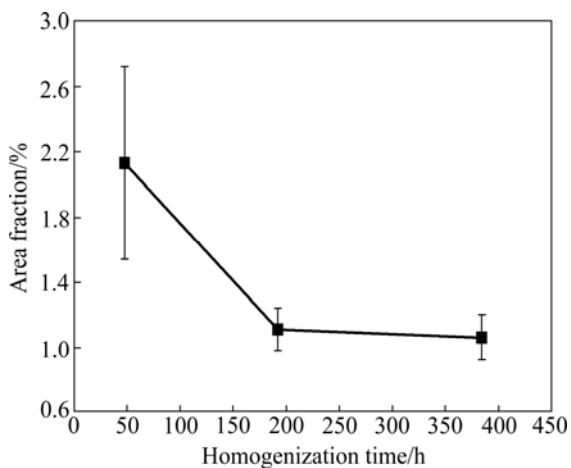


Fig. 2 Optical micrographs of specimens homogenized for different time: (a) 48 h; (b) 384 h



**Fig. 3** SEM images and EDX results of specimens homogenized for different time: (a, b) 48 h; (c) 192 h; (d) 384 h; (e) EDX spectrum of particle *A* in Fig. 3(a); (f) EDX spectrum of particle *B* in Fig. 3(b)



**Fig. 4** Influence of homogenization time on area fraction of second phase in homogenized specimens

not uniform for 384 h. The area fraction seemed to increase first and then decrease with the increase of homogenization time, and the maximum value was observed after homogenization for 192 h. This may imply that coarsening of  $\text{Al}_3\text{Zr}$  dispersoids occurred after homogenization for 384 h.

Figure 7 shows typical TEM images of the samples at  $d=3$  mm and 78 mm in the end-quenched and aged specimens. At  $d=3$  mm in the end-quenched specimen homogenized for 48 h, apart from the round  $\text{Al}_3\text{Zr}$  dispersoids, a high density of fine  $\eta'$  strengthening precipitates could be seen in the matrix (see Fig. 7(a)). But the density of  $\text{Al}_3\text{Zr}$  dispersoids seems to be lower than that shown in Fig. 5(a). This may be because the strong coherent distortion due to  $\eta'$  strengthening

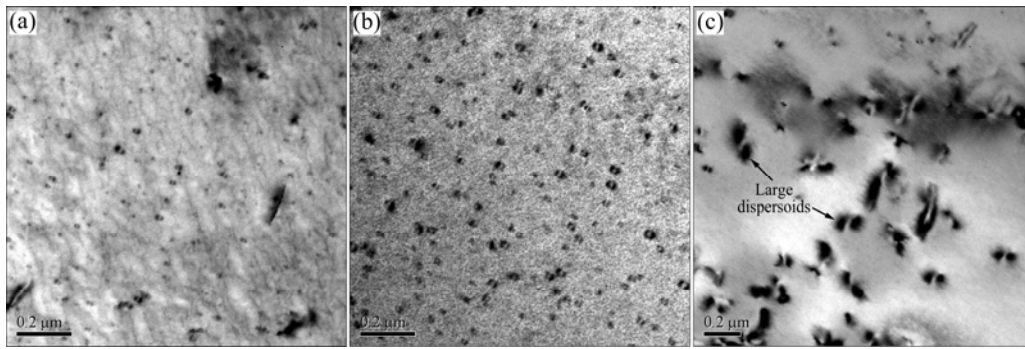


**Fig. 5** TEM images showing  $\text{Al}_3\text{Zr}$  dispersoids in specimens homogenized for different time: (a) 48 h; (b) 192 h; (c) 384 h

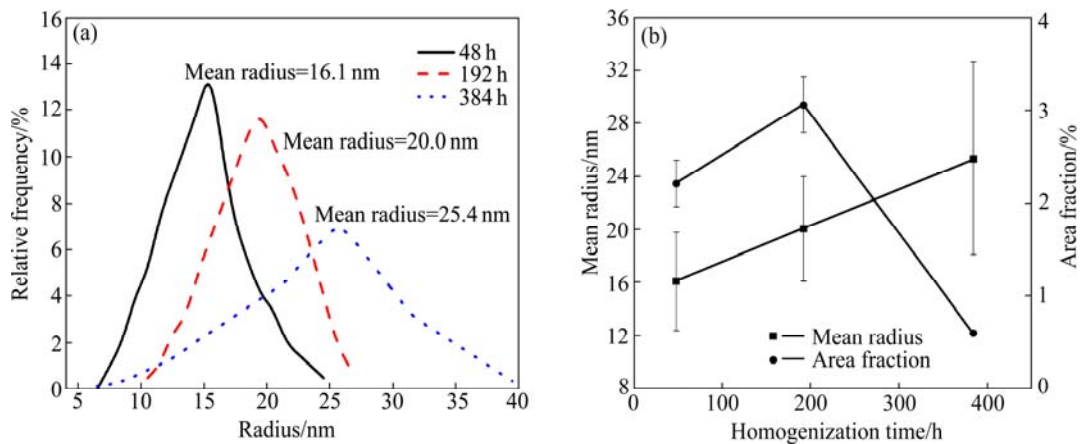


**Fig. 6** Character of  $\text{Al}_3\text{Zr}$  dispersoids in specimens homogenized for different time: (a) Size distribution; (b) Mean radius and area fraction

precipitates made it difficult to reveal small  $\text{Al}_3\text{Zr}$  dispersoids, and only some large  $\text{Al}_3\text{Zr}$  dispersoids could be observed. In the sample at  $d=78$  mm (Fig. 7(b)), apart from  $\text{Al}_3\text{Zr}$  dispersoids and  $\eta'$  strengthening precipitates in the matrix, some rod-like  $\eta$  phase particles were visible and associated with  $\text{Al}_3\text{Zr}$  dispersoids. In the specimen homogenized for 192 h, a similar phenomenon could be observed, as shown in Fig. 7(c). In the specimen homogenized for 384 h, however, there were more quench-induced  $\eta$  phase particles in the matrix (see Fig. 7(d)). Combining with Fig. 5(c), it is likely that most  $\text{Al}_3\text{Zr}$  dispersoids acted as nucleation sites for  $\eta$  phase during slow quenching. The size of these  $\eta$  phase particles was about 65 nm.

#### 4 Discussion

According to the hardness curves and hardness retention curves in Fig. 1, it is likely that quench sensitivity tends to increase slightly with the increase of homogenization time. From the microstructural images shown in Figs. 2–7, the amount of grain boundaries, which often act as preferential nucleation sites for  $\eta$  phase during slow quenching, was not changed. Therefore, it is thought that there are two factors

responsible for the slightly higher quench sensitivity. One is the large amount of Zn, Mg and Cu solutes in the matrix, and the other is the change in character of  $\text{Al}_3\text{Zr}$  dispersoids.

After homogenization from 48 h to 192 h,  $T$  phase was dissolved completely (Figs. 3 and 4). 7085 aluminum alloy is an age hardenable alloy, and the hardness after aging is related to the volume fraction of strengthening precipitates, which is determined by the amount of Zn and Mg in the matrix [21]. Dissolution of  $T$  phase can increase the amount of Zn, Mg and Cu in the solid solution and thus hardness is higher after aging. This may also be proved from Fig. 1, where the hardness was increased from about HV 169 for 48 h to HV 175 for 192 h and to HV 176 for 384 h at  $d=3$  mm from the water-cooled end. However, quench sensitivity was increased as well because a higher concentration of Zn, Mg, Cu can prompt the precipitation of  $\eta$  phase during slow quenching [6,22], therefore, the amount of alloying elements available for strengthening precipitates during subsequent aging was decreased, resulting in lower hardness. Meanwhile, the size and area fraction of  $\text{Al}_3\text{Zr}$  dispersoids were increased (Figs. 5 and 6). Larger dispersoids are less coherent with the matrix [20], and the interfacial energy is higher. Consequently, more

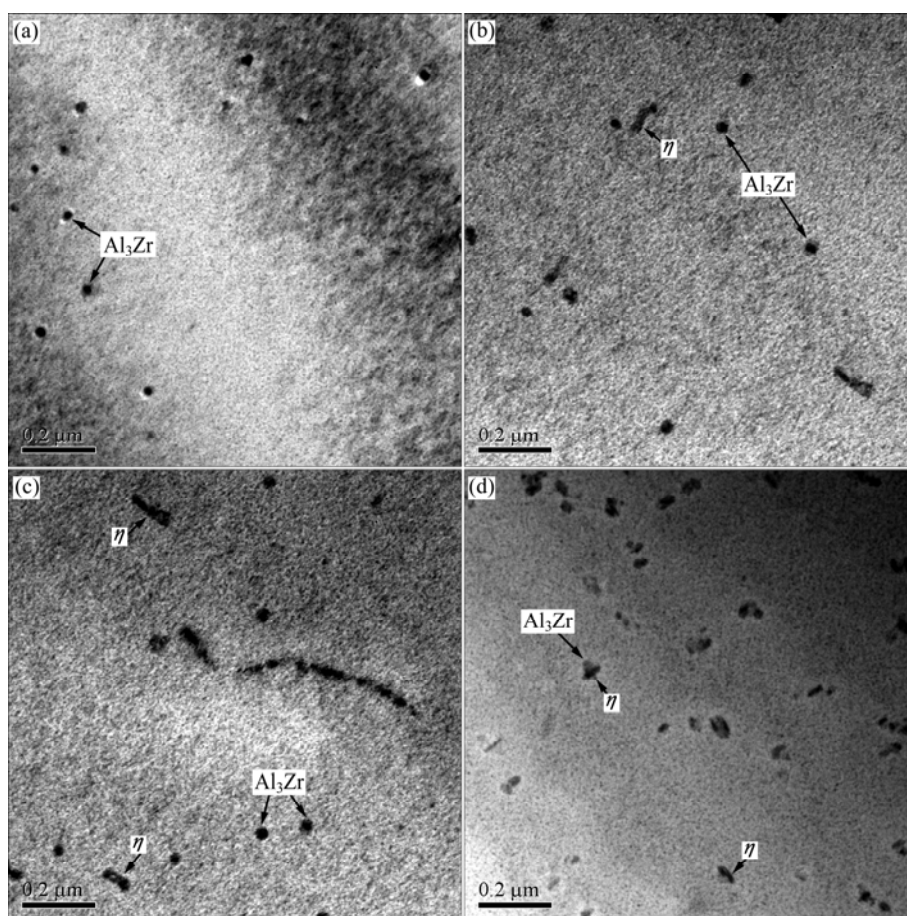


**Fig. 7** TEM images at different locations in end-quenched and aged specimens homogenized for different time: (a)  $d=3$  mm, 48 h; (b)  $d=78$  mm, 48 h; (c)  $d=78$  mm, 192 h; (d)  $d=78$  mm, 384 h

dispersoids tended to act as nucleation sites for heterogeneous precipitation of  $\eta$  phase during slow quenching, leading to loss of solutes in the solid solution (Fig. 7). This may also be responsible for higher quench sensitivity. But it is still difficult to distinguish the contribution due to the change in the concentration of Zn, Mg, Cu or due to the change in the character of  $\text{Al}_3\text{Zr}$  dispersoids. With the further increase of homogenization time to 384 h, an equilibrium state might be obtained, as soluble  $T$  phase was dissolved completely after about 192 h. In other words, the concentration of Zn, Mg, Cu in the solid solution was not further increased. So the change in quench sensitivity was caused by the change in character of  $\text{Al}_3\text{Zr}$  dispersoids only. Most  $\text{Al}_3\text{Zr}$  dispersoids became larger, so the interfacial energy was higher for the interface between them and the matrix, which can prompt the formation of  $\eta$  phase during slow quenching. But the size of these quench-induced  $\eta$  phase was quite small, and thus had slight influence on hardness after aging. A similar phenomenon was observed in a cast sample of 7055 aluminum alloy [3]. Consequently, quench sensitivity was slightly increased as the drop percentage in hardness was increased from 6.2% to 6.9% (Fig. 1(b)), and the change in the character

of  $\text{Al}_3\text{Zr}$  dispersoids exerted slight influence on quench sensitivity.

## 5 Conclusions

1) Quench sensitivity of the homogenized 7085 aluminum alloy increased slightly with the increase of homogenization time from 48 h to 384 h, as the largest difference in hardness in the end-quenched and aged specimen was 5.2% and 6.9%, respectively.

2) Prolonging homogenization time had little effect on grain structure, but improved the dissolution of soluble  $T$  phase, which increased the concentration of Zn, Mg and Cu in the solid solution, and resulted in larger  $\text{Al}_3\text{Zr}$  dispersoids, which tended to prompt the formation of  $\eta$  phase inside grains during slow quenching. With the homogenization time increasing from 192 h to 384 h, the change in the character of  $\text{Al}_3\text{Zr}$  dispersoids exerted only slight influence on quench sensitivity.

## References

- [1] BOSELLI J, CHAKRABARTI D J, SHUEY R T. Aerospace applications: Metallurgical insights into the improved performance of

- aluminum alloy 7085 thick products [C]/HIRSCH J, SKROTZKI B, GOTTSTEIN G. Aluminium alloys: Their Physical and Mechanical Properties. Proceedings of the 11 International Conference on Aluminium alloys. Aachen, Germany, 2008: 202–208.
- [2] CHAKRABARTI D J, LIU J, SAWTELL R R, VENEMA G B. New generation high strength high damage tolerance 7085 thick alloy product with low quench sensitivity [J]. Materials Forum, 2004, 28: 969–974.
- [3] LIU S D, LIU W J, ZHANG Y, ZHANG X M. Effect of microstructure on the quench sensitivity of AlZnMgCu alloys [J]. Journal of Alloys and Compounds, 2010, 507(1): 53–61.
- [4] CHEN Song-yi, CHEN Kang-hua, PENG Guo-sheng, LIANG Xin, CHEN Xue-hai. Effect of quenching rate on microstructure and stress corrosion cracking of 7085 aluminum alloy [J]. Transactions of Nonferrous Metals Society of China, 2012, 22(1): 47–52.
- [5] ROBINSON J S, CUDD R L, TANNER T D. Quench sensitivity and tensile property inhomogeneity in 7010 forgings [J]. Journal of Materials Processing Technology, 2001, 119(1–3): 261–267.
- [6] LIM S T, YUN S J, NAM S W. Improved quench sensitivity in modified aluminum alloy 7175 for thick forging applications [J]. Materials Science and Engineering A, 2004, 371(1–2): 82–90.
- [7] LI Pei-yue, XIONG Bai-qing, ZHANG Yong-an, LI Zhi-hui, ZHU Bao-hong. Quench sensitivity and microstructure character of high strength AA7050 [J]. Transactions of Nonferrous Metals Society of China, 2012, 22(2): 268–274.
- [8] TANG Jian-guo, CHEN Hui, ZHANG Xin-ming. Influence of quench-induced precipitation on aging behavior of Al–Zn–Mg–Cu alloy [J]. Transactions of Nonferrous Metals Society of China, 2012, 22(6): 1255–1263.
- [9] ZHANG X M, LIU W J, LIU S D, ZHOU M Z. Effect of processing parameters on quench sensitivity of an AA7050 sheet [J]. Materials Science and Engineering A, 2011, 528(3): 795–802.
- [10] GODARD D, ARCHAMBAULT P, AEBY-GAUTIER E. Precipitation sequences during quenching of the AA7010 alloy [J]. Acta Materialia, 2002, 50(9): 2319–2329.
- [11] LIU Sheng-dan, ZHANG Yong, LIU Wen-jun, DENG Yun-lai, ZHANG Xin-ming. Effect of step-quenching on microstructure of aluminum alloy 7055 [J]. Transactions of Nonferrous Metals Society of China, 2010, 20(1): 1–6.
- [12] LIU Wen-jun. Investigation on precipitation behavior during quenching and quench sensitivity of Al–Zn–Mg–Cu alloy [D]. Changsha: Central South University, 2011. (in Chinese)
- [13] LU Yan-hong. Influence of homogenization treatment on the microstructures and mechanical properties of the aluminum alloy 7055 [D]. Changsha: Central South University, 2012. (in Chinese)
- [14] DONS A L. The alstruc homogenization model for industrial aluminum alloys [J]. Journal of Light Metals, 2001, 1(2): 133–149.
- [15] ROBSON J D. Microstructural evolution in aluminium alloy 7050 during processing [J]. Materials Science and Engineering A, 2004, 382(1–2): 112–121.
- [16] LIU Wen-jun, ZHANG Xin-ming, LIU Sheng-dan, ZHOU Xin-wei. Effect of homogenization on quenching sensitivity of 7050 aluminum alloy plates [J]. The Chinese Journal of Nonferrous Metals, 2010, 20(6): 1102–1109. (in Chinese)
- [17] LIU Sheng-dan, LI Cheng-bo, DENG Yun-lai, ZHANG Xin-ming. Influence of aging on the hardenability of 7055 aluminum alloy thick plate [J]. Acta Metallurgica Sinica, 2012, 48(3): 343–350. (in Chinese)
- [18] LIU S D, LI C B, YUAN Y B, ZHANG X M. Influence of cooling rate after homogenization on the microstructure and mechanical properties of 7050 aluminum alloy [J]. Metals and Materials International, 2012, 18(4): 679–683.
- [19] MONDAL C, MUKHOPADHYAY A K. On the nature of T(Al<sub>2</sub>Mg<sub>3</sub>Zn<sub>3</sub>) and S(Al<sub>2</sub>CuMg) phases present in as-cast and annealed 7055 aluminum alloy [J]. Materials Science and Engineering A, 2005, 391(1–2): 367–376.
- [20] KNIPLING K E. Development of a nanoscale precipitation creep-resistant aluminum alloy containing trialuminide precipitates [D]. Evanston: Northwestern University, 2006.
- [21] CHEN K H, LIU H W, ZHANG Z. The improvement of constituent dissolution and mechanical properties of 7055 aluminum alloy by stepped heat treatments [J]. Journal of Materials Processing Technology, 2003, 142(1): 190–196.
- [22] DENG Y L, WANG L, ZHANG Y Y. Influence of Mg content on quench sensitivity of Al–Zn–Mg–Cu aluminum alloys [J]. Journal of Alloys and Compounds, 2011, 509 (13): 4636–4642.

## 均匀化时间对 7085 铝合金淬火敏感性的影响

郑玉林<sup>1,2</sup>, 李承波<sup>1,3</sup>, 刘胜胆<sup>1,3</sup>, 邓运来<sup>1,3</sup>, 张新明<sup>1,3</sup>

1. 中南大学 材料科学与工程学院, 长沙 410083;

2. 广西南南铝业公司, 南宁 530000;

3. 中南大学 有色金属材料科学与工程教育部重点实验室, 长沙 410083

**摘要:** 采用末端淬火实验、光学显微镜(OM)、扫描电镜(SEM)和透射电镜(TEM)研究均匀化时间对 7085 铝合金淬火敏感性的影响。结果表明, 均匀化时间从 48 h 延长至 384 h, 淬火敏感性有所增加, 端淬试样经人工时效后硬度的最大差值从 5.2% 增加到 6.9%。均匀化时间延长对晶粒组织没有影响, 但促使  $T$  相的溶解, 增加 Al<sub>3</sub>Zr 弥散粒子的尺寸, 减小其密度。慢速淬火时, 在晶内的 Al<sub>3</sub>Zr 弥散粒子上能观察到一些尺寸较小的淬火析出  $\eta$  相, 这降低了时效后的硬度。Al<sub>3</sub>Zr 粒子特征的变化对淬火敏感性影响很小。

**关键词:** 7085 铝合金; 均匀化; 末端淬火; 淬火敏感性; Al<sub>3</sub>Zr 弥散粒子; 平衡  $\eta$  相

(Edited by Sai-qian YUAN)